Practical techniques for time-lapse AVO inversion

A. Nassir Saeed, Laurence R. Lines, and Gary F. Margrave

ABSTRACT

Successful prediction and mapping of fluid saturation and pressure changes in hydrocarbon reservoir depends mainly on accurate relative amplitude processing of seismic data vintages that meet AVO complaints as well as a practical time-lapse AVO inverse scheme.

In this report, several time-lapse AVO inverse schemes are proposed in order to improve estimation of elastic physical model parameters, provide better inverse section in presence of noise and prove their robustness in terms of time calculation and estimation of the change in model parameter estimation.

Inversion of seismic reflectivity difference only of time-lapse seismic data surveys is a quick method in time-lapse AVO inversion. Sequential cross-reflectivity constraint inversion is a robust time-lapse AVO inversion schemes that can be implemented to constraint noise effect on the data and to ensure smooth change in estimating reservoir attributes from time-lapse inversion.

Total inversion of the differences schemes are other time-lapse AVO inverse techniques that can be carried out into two different inverse objectives. These are: Inverting of time-lapse AVO seismic data for estimating of elastic physical model parameters of monitoring line and time-lapse reflectivity model parameters changes of base and monitoring lines. While a second total inversions of differences can be implemented to estimate elastic physical model parameters of base line along with time-lapse reflectivity model parameters changes of base and monitoring lines.

The proposed time-lapse inverse schemes in this report are tested on synthetic seismic data. These proposed inverse techniques are to be tested using real time-lapse seismic data from Pikes-Peak heavy oil fields that are being processed for AVO complaints and optimal repeatability.

INTRODUCTION

In reservoir monitoring, the differences in seismic attributes of the base and monitor surveys data are used in evaluating the spatial changes of reservoir attributes (LandrØ, 2001) after reservoir being depleted due to production process.

A common conventional method used in time-lapse AVO inversion, is to invert seismic data of base and monitor surveys separately (Watson, and Lines, 2001; Zou, 2005) and then study the difference or percentage changes of estimating model parameters of time-lapse survey. Another method that probably depends on the size of time-lapse seismic data vintages as well as on commercial software or in-house developed software(Gray, 2011; personal communication), is to perform simultaneous inversion of base and monitor seismic data so as to reduce time-calculations.

In this report, more practical and non-conventional inverse techniques for time lapse AVO inversion are presented in this study. The objectives from these inverse techniques are to enhance model parameters estimations, taken into our consideration presence of noise, and prove their robustness in terms of accuracy and time calculations.

THEORY OF TIME-LAPSE AVO INVERSION

For given two data sets, says (base, $\mathbf{d_0}$, and a monitor, $\mathbf{d_1}$,), synthetic reflectivity data can be written as:

$$\mathbf{d_0}=\mathbf{G_0}\ \mathbf{m_0} \quad \text{for base line} \tag{1}$$
$$\mathbf{d_1}=\mathbf{G_1}\ \mathbf{m_1} \quad \text{for monitoring line} \tag{2}$$

where,

d is data, **G** is forward or operator, and **m** is unknown reflectivity model parameters sought.

The Least squares inverse problems requires minimization of cost functions below

$$J(m_0) = \|\boldsymbol{G_0 m_0} - \boldsymbol{d_0}\|^2 + \lambda^2\|\boldsymbol{G_0 m_0}\|^2 \tag{3}$$
$$J(m_1) = \|\boldsymbol{G_1 m_1} - \boldsymbol{d_1}\|^2 + \lambda^2\|\boldsymbol{G_1 m_1}\|^2 \tag{4}$$

which give the solutions

$$m_0 = (\boldsymbol{G_0^T} G_0 + \lambda^2 \boldsymbol{R_0^T} R_0)\boldsymbol{G_0^T d_0} \tag{5}$$

$$m_1 = (\boldsymbol{G_1^T} G_1 + \lambda^2 \boldsymbol{R_1^T R_1})\boldsymbol{G_1^T d_1} \tag{6}$$

where,

R and **λ** are regularization operator and parameter (constable et al., 1987) respectively.

In the time-lapse AVO inversion, Δ**m** is then computed either as the difference between estimated base and monitor model parameters

$$\boldsymbol{\Delta m = m_1 - m_0} \tag{7}$$

Or as percentage of changes between base and monitoring model parameters

$$\boldsymbol{\Omega_m = \frac{\Delta m}{m_0}.100} \tag{8}$$

Figures (1 and 2) show inversion of synthetic data for base and monitoring models (Saeed, et al., 2010a) that were carried out separately as common procedure for time-lapse AVO inversion.

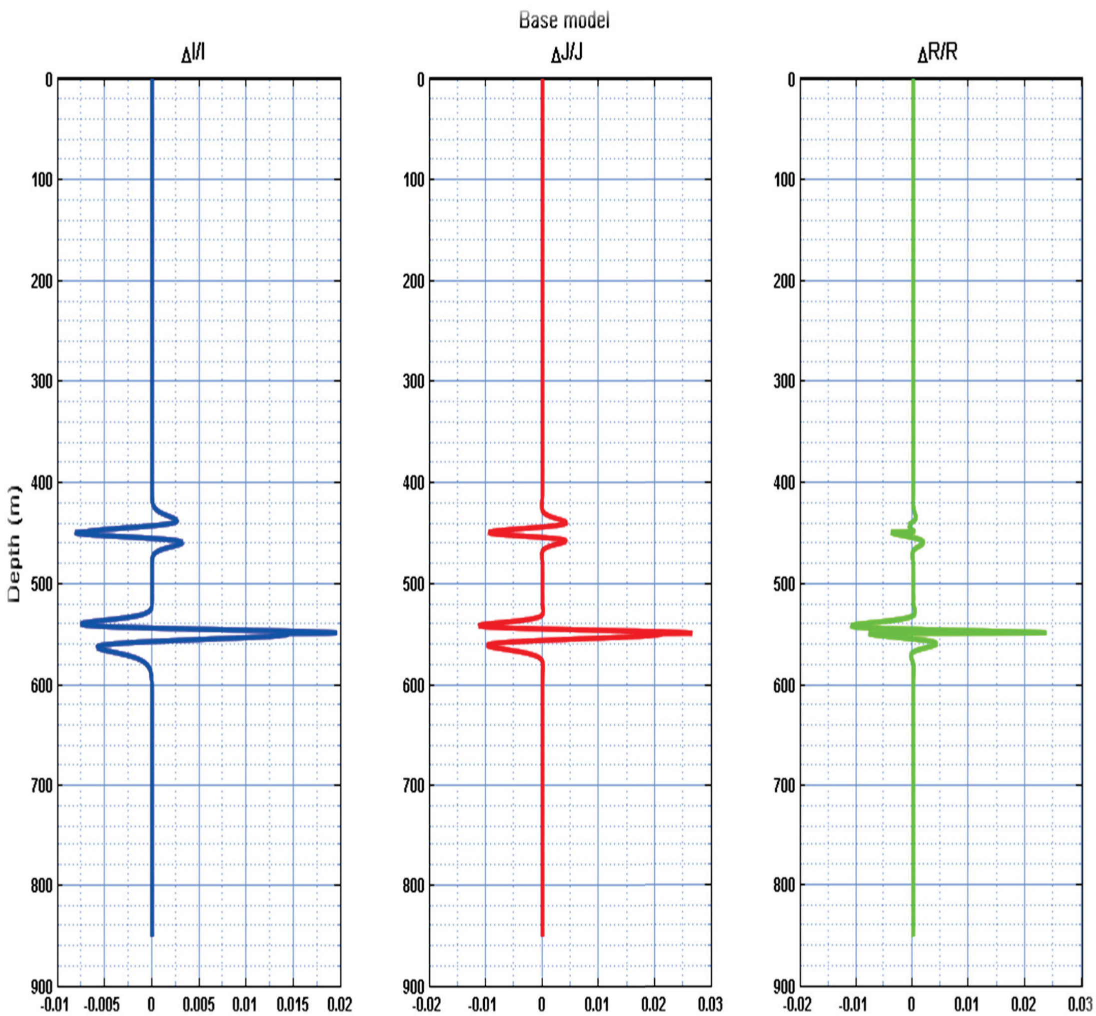

FIG.1 Estimated model parameters for $\frac{\Delta I}{I}$, $\frac{\Delta J}{J}$ and $\frac{\Delta R}{R}$ of the **base** synthetic data of time-lapse model. Note that band-limited low-frequency of log is not included

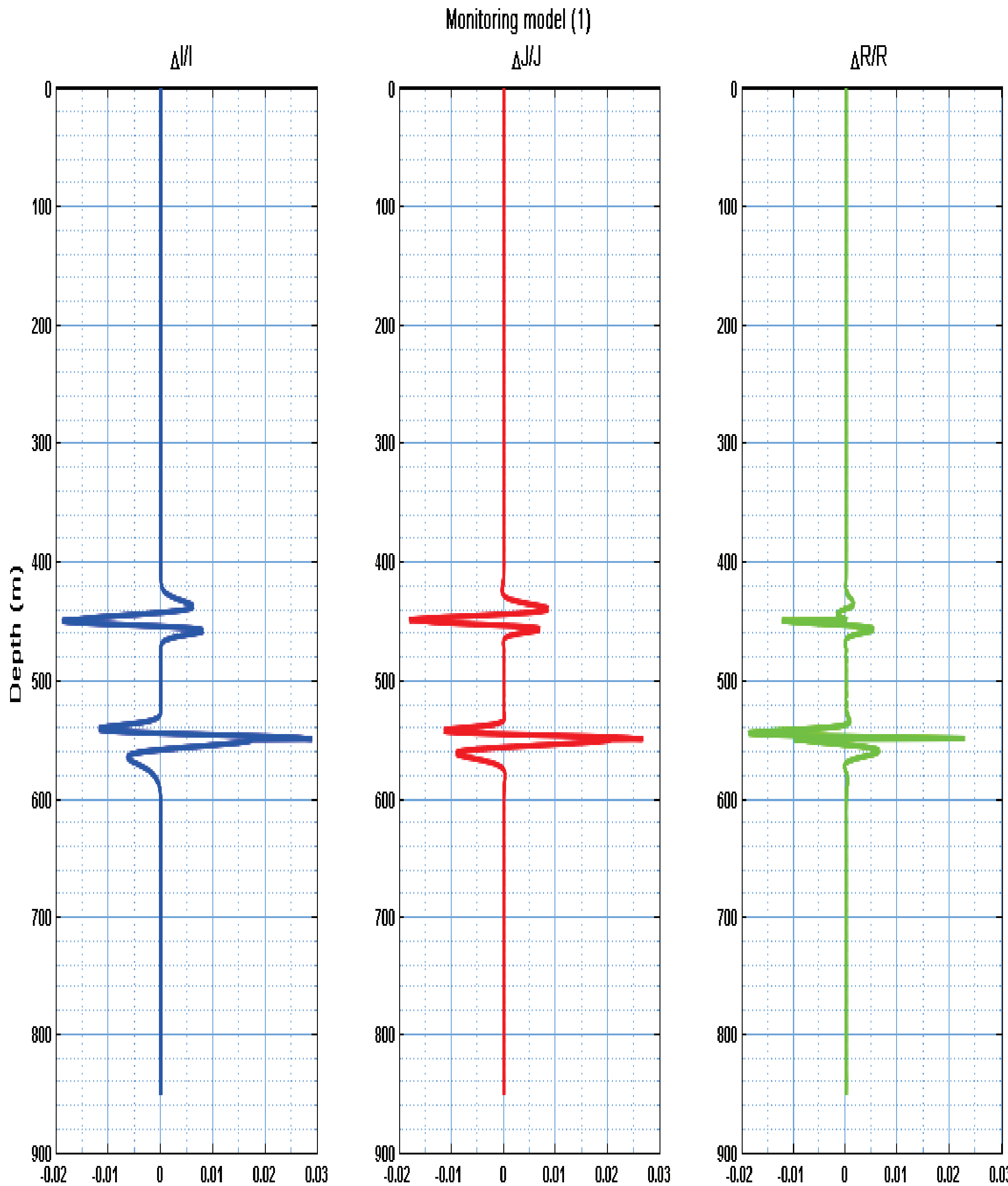

FIG.2 Estimated model parameters ($\frac{\Delta I}{I}$, $\frac{\Delta J}{J}$ and$\frac{\Delta R}{R}$) of the **monitoring model-1** of time-lapse model. Note that band-limited low-frequency of log is not included

In the following subsections, several practical time-lapse AVO inversion schemes are presented.

Inversion of total differences: *Inverting for monitoring line,* $\mathbf{m_1}$*, and time-lapse reflectivity model parameters,* $\boldsymbol{\Delta m}$

inversion of time-lapse data for estimating model parameters of monitoring line and time-lapse reflectivity model changes is accomplished by taking the difference between equations (1 and 2) and then re-arranging them yields,

$$\mathbf{G_1\, m_1 - G_0\, m_0 = d_1 - d_0} \qquad (9)$$

Then, by using $\mathbf{\Delta G} = \mathbf{G_1} - \mathbf{G_0}$, and substitute for $\boldsymbol{G_1}$, equation (9) can be written as

$$(\Delta \mathbf{G} + \mathbf{G_0})\, \mathbf{m_1} - \mathbf{G_0\, m_0} = \Delta \mathbf{d} \qquad (10)$$

Re-arranging (10), yields

$$\Delta \mathbf{G m_1} + \mathbf{G_0} \Delta \mathbf{m} = \Delta \mathbf{d} \qquad (11)$$

In augmented matrix notation, cost functions (3 and 4) can be joint - inverted, and written as

$$J(m_1, \Delta \mathrm{m}) = \left\| \begin{bmatrix} \Delta \mathbf{G} & \mathbf{0} \\ \mathbf{0} & \boldsymbol{G_0} \end{bmatrix} \begin{bmatrix} \boldsymbol{m_1} \\ \Delta \mathbf{m} \end{bmatrix} - \begin{bmatrix} \boldsymbol{d_1} \\ \boldsymbol{d_0} \end{bmatrix} \right\|^2 + \left\| \begin{bmatrix} \lambda^2 \boldsymbol{R_1^T R}_1 & \mathbf{0} \\ \mathbf{0} & \lambda^2 \boldsymbol{R_0^T} R_0 \end{bmatrix} \begin{bmatrix} \boldsymbol{m_1} \\ \Delta \mathbf{m} \end{bmatrix} \right\|^2 \qquad (12)$$

Inversion of total differences: *Inverting for base line,* $\mathbf{m_0}$*, and time-lapse reflectivity model parameters,* $\boldsymbol{\Delta m}$

It would be more acceptable, if we directly invert for the base line reflectivity model parameters, $\boldsymbol{m_0}$, and time-lapse reflectivity model parameters $\boldsymbol{\Delta m}$ by using the following substitution for $\boldsymbol{m_1}$ in equation (9),

$$\boldsymbol{\Delta m} + \boldsymbol{m_0} = \boldsymbol{m_1} \qquad (13)$$

Equation (9) then can be re-written as

$$\mathbf{G_1}\, (\boldsymbol{\Delta m} + \boldsymbol{m_0}) - \mathbf{G_0\, m_0 = d_1 - d_0} \qquad (14)$$
$$\mathbf{G_1}\, \boldsymbol{\Delta m} + \mathbf{G_1}\, \boldsymbol{m_0} - \mathbf{G_0\, m_0 = d_1 - d_0} \qquad (15)$$

$$\Delta\mathbf{G}\boldsymbol{m_0} + \mathbf{G1}\ \boldsymbol{\Delta m} = \mathbf{d_1} - \mathbf{d_0} \tag{16}$$

$$\Delta\mathbf{d} = \mathbf{d_1} - \mathbf{d_0} \tag{17}$$

$$\Delta\mathbf{G}\boldsymbol{m_0} + \mathbf{G1}\ \boldsymbol{\Delta m} = \Delta\mathbf{d} \tag{18}$$

Then, in augmented matrix notation, cost functions (3 and 4) for inverting for base line, m_0, and time-lapse reflectivity model parameters, $\Delta\mathrm{m}$ is written as

$$J(m_0, \Delta\mathrm{m}) = \left\| \begin{bmatrix} \Delta\mathbf{G} & \mathbf{0} \\ \mathbf{0} & \boldsymbol{G_1} \end{bmatrix} \begin{bmatrix} \boldsymbol{m_0} \\ \Delta\mathbf{m} \end{bmatrix} - \begin{bmatrix} \boldsymbol{d_0} \\ \boldsymbol{d_1} \end{bmatrix} \right\|^2 + \left\| \begin{bmatrix} \lambda^2 \boldsymbol{R_0^T R}_0 & \mathbf{0} \\ \mathbf{0} & \lambda^2 \boldsymbol{R_1^T} R_1 \end{bmatrix} \begin{bmatrix} \boldsymbol{m_0} \\ \Delta\mathbf{m} \end{bmatrix} \right\|^2 \tag{19}$$

Or

$$J(m_0, \Delta\mathrm{m}) = \left\| \begin{bmatrix} \boldsymbol{G_1} & \boldsymbol{G_0} \\ \mathbf{0} & \boldsymbol{G_1} \end{bmatrix} \begin{bmatrix} \boldsymbol{m_0} \\ \Delta\mathbf{m} \end{bmatrix} - \begin{bmatrix} \boldsymbol{d_0} \\ \boldsymbol{d_1} \end{bmatrix} \right\|^2 + \left\| \begin{bmatrix} \lambda^2 \boldsymbol{R_0^T R}_0 & \mathbf{0} \\ \mathbf{0} & \lambda^2 \boldsymbol{R_1^T} R_1 \end{bmatrix} \begin{bmatrix} \boldsymbol{m_0} \\ \Delta\mathbf{m} \end{bmatrix} \right\|^2 \tag{20}$$

Inversion of differences of data ($\boldsymbol{\Delta d}$) only

The inversion of differences of data only is considered a quick inverse scheme to estimate the change in elastic model parameters. This method is based on assumption that if there is a change in $\mathbf{d}_{\text{diff}}$ of equation (21), this will yield a change in estimated $\Delta\mathbf{m}$. However, if there is no change in $\mathbf{d}_{\text{diff}}$ then $\Delta\mathbf{m} = \mathbf{0}$ at that specific depth interval. Figure (3), is application of equation (21) to time-lapse model (Saeed, et al., 2010a).

$$\left(\left[\mathbf{G}^{\mathsf{T}}\mathbf{G} + \lambda\, \mathbf{W}_{\mathbf{m}}^{\mathsf{T}}\mathbf{W}_{\mathbf{m}} \right) \right] \Delta\mathbf{m} = \mathbf{G}^{\mathsf{T}}\mathbf{d}_{\text{diff}} \tag{21}$$

In real field data, we would rarely get $\mathbf{d}_{\text{diff}} = 0$ for a specific depth interval. However, we would rather have very small change; say 0.0005 that not necessarily due to fluid change. These very small values of changes can be attributed to the geometry difference between time-lapse surveys or random noise or even processing differences.

Therefore, we can set a *cut-off point* whereby we assume any value differences, $\mathbf{d}_{\text{diff}}$, in the data at that specific depth interval equal or below that *cut-off point* can then be set to zero,. Thus, resulting differences would be more representative of fluid change.

The accuracy of inversion of differences of data inverse scheme above will have to be tested using real field data. Then, we need to compare results from this inversion scheme with ones from inverting time-lapse data separately.

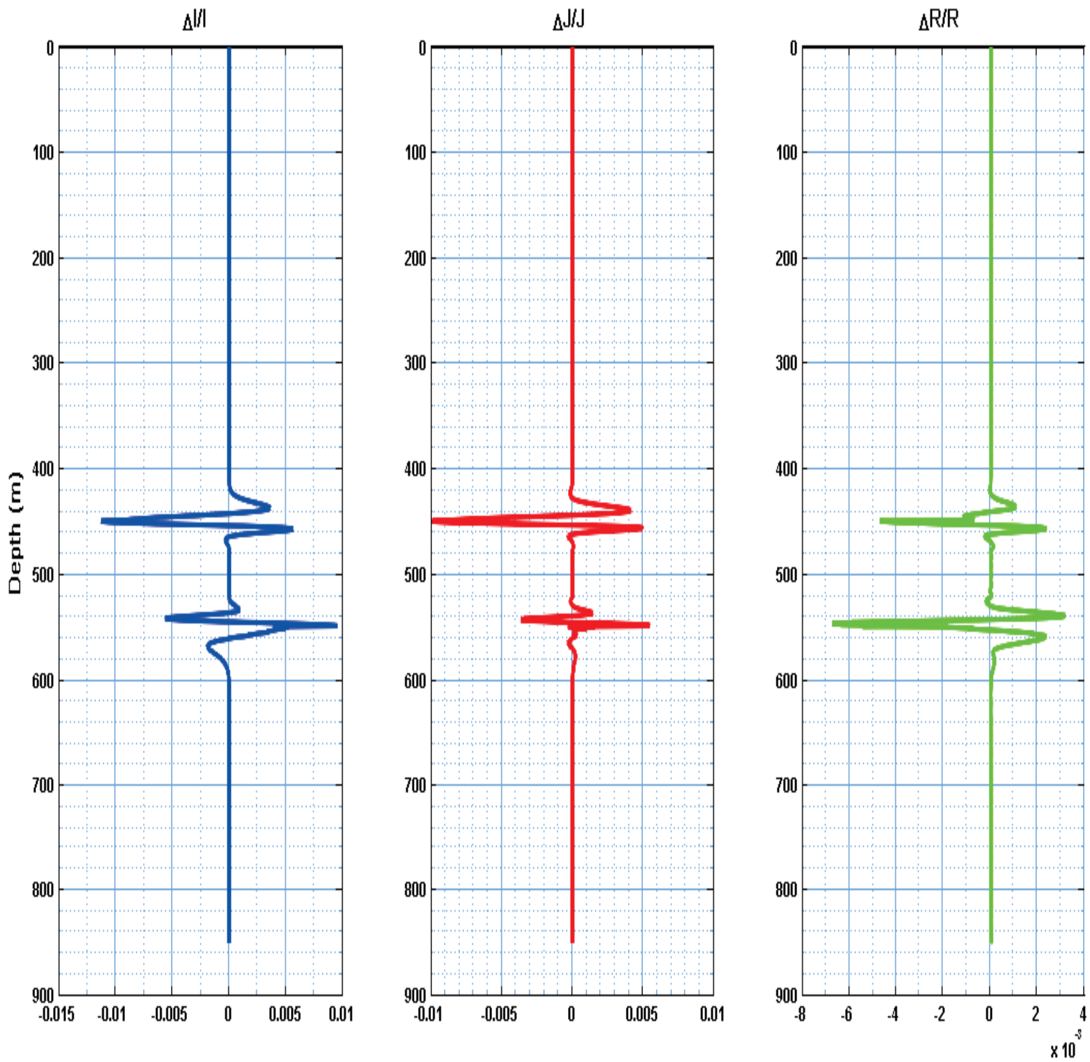

FIG.3. Estimated model parameters using the difference in data, $\mathbf{d}_{diff}$, only.

Robust time-lapse AVO inversion

In geophysical inversion, Constraints or often called, robustness, can be incorporated in inverse problem in order to refine estimated model parameters; thus enhance obtained inverse model . Constraints can be incorporated in either data spaces (Bube and Langan, 1997; Saeed et. al., 2010b) or in model spaces (Ajo-Franklin et. al., 2007; Saeed et al., 2010c) or in both space domains, which is often called blocky inversion (Claerbout, and Muir, 1973).

In Pikes-Peak time-lapse seismic surveys, noise is more noticeable in some of shot gathers of the monitoring seismic survey, 2000, compared to the base seismic survey, 1991. These noises are due to jack pumps that were operating during the course of seismic data acquisition. In order to simulate the effect of jack pump noise in time-lapse model, random noise were added to part of synthetic data of monitoring model (Figures 4).

The *sequential cross-reflectivity constraint inversion* in equation (22) is one form of robust time-lapse inversion method whereby estimated model parameters of base survey are used to constraint inversion of monitoring model so as to ensure smooth change in estimated elastic model parameters of monitoring model.

$$[(\boldsymbol{G^T G} + \boldsymbol{\lambda_1 W_m^T W_m} + \boldsymbol{\lambda_2 V^T V})]\boldsymbol{m_i} = \left[\boldsymbol{G^T d} + \boldsymbol{\lambda_2 V^T V}(\boldsymbol{m_{i-1}^M} - \boldsymbol{m_{i-1}^B})^{\boldsymbol{T}}\right] \quad (22)$$

where,

$$\boldsymbol{V_{monit.}} = diag\left[\Delta\left(\boldsymbol{m_{i-1}^M} - \boldsymbol{m_0^B}\right)\right]$$

Because $\boldsymbol{V}$ and $(\boldsymbol{m_{i-1}^M} - \boldsymbol{m_{i-1}^B})^{\boldsymbol{T}}$are functions of unknown *base and monitor model parameters,* this is a non-linear system, and iterative approach must be used. This is referred to iteratively re-weighted least squares, IRLS, (Wolke and Schwetlick, 1988).

We followed the approach of Farquharson and Oldenburg, (1998), by setting ***V*** and $(\boldsymbol{m_{i-1}^M} - \boldsymbol{m_{i-1}^B})^{\boldsymbol{T}}$= ***I*** for the first iteration, which result in traditional least squares solution. The estimation of $\boldsymbol{m_i^B}$ for i=1 is then subsequently substituted again in equation (22) to obtain a new $\boldsymbol{m_{i+1}^M}$. The procedure is repeated until the estimated model parameters of monitoring survey between successive IRLS iterations becomes less than tolerance value, τ given in convergence limit equation (23).

$$\frac{\left\|m^{k+1} - m^k\right\|_2}{1 + \left\|m^{k+1}\right\|_2} \langle \tau \quad (23)$$

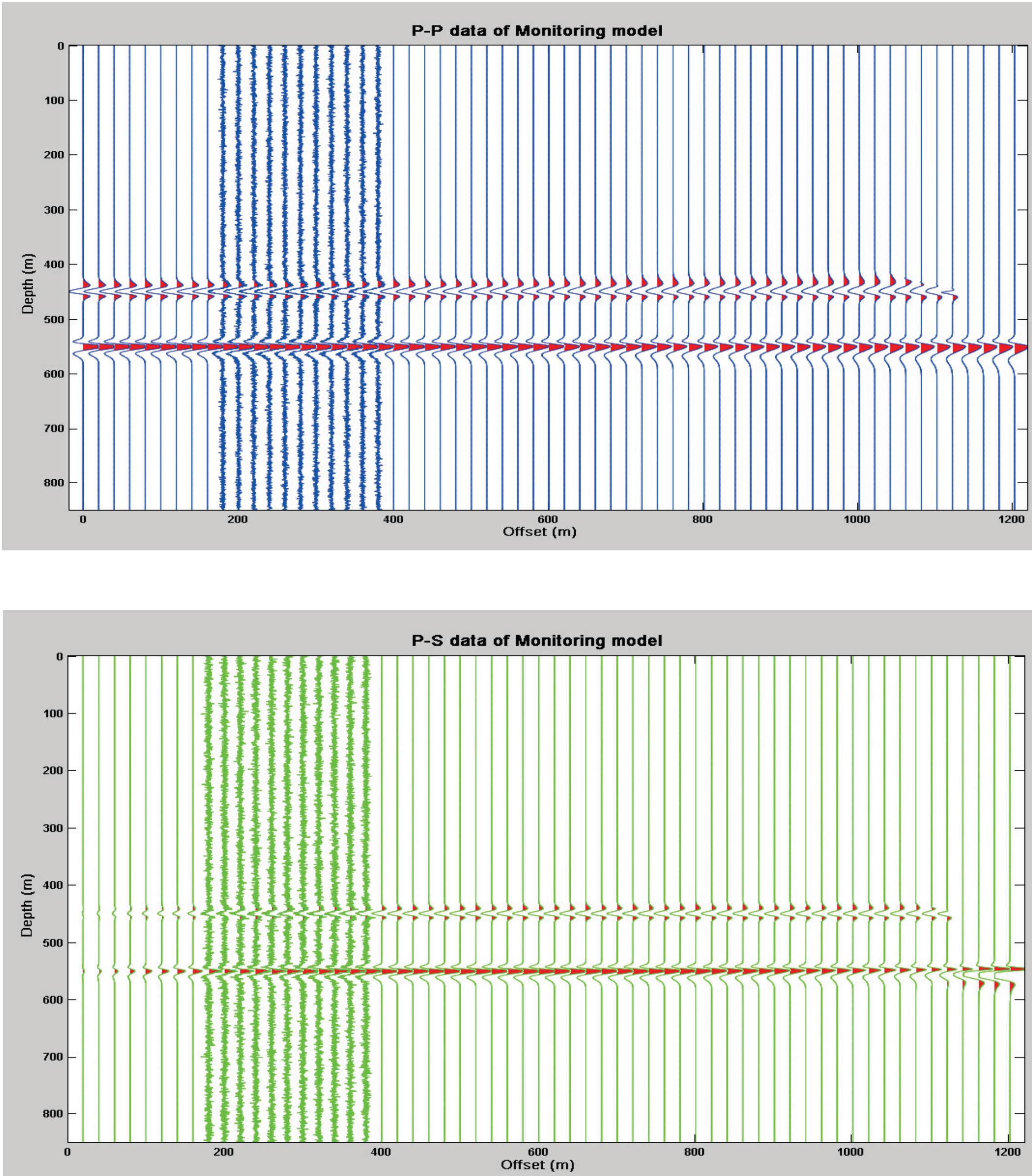

FIG.4. Synthetic P-P and P-S section of monitoring model with noise added.

Figure (5) shows measure and inverted acoustic impedances for the monitoring model using cross-reflectivity constraint (robust time-lapse) inverse scheme. Figure (6) shows regularization parameter during the inversion while figure (7) shows the RMS error during inversion. Note that band limited low frequency of well log was not added to inverted model parameters attributes and better correlation to measured acoustic impedance would be achieved if these band-limited low frequencies were added. The band-limit low frequency function of Ferguson and Margrave, (1996) is being modified to accommodate time-lapse AVO inversion.

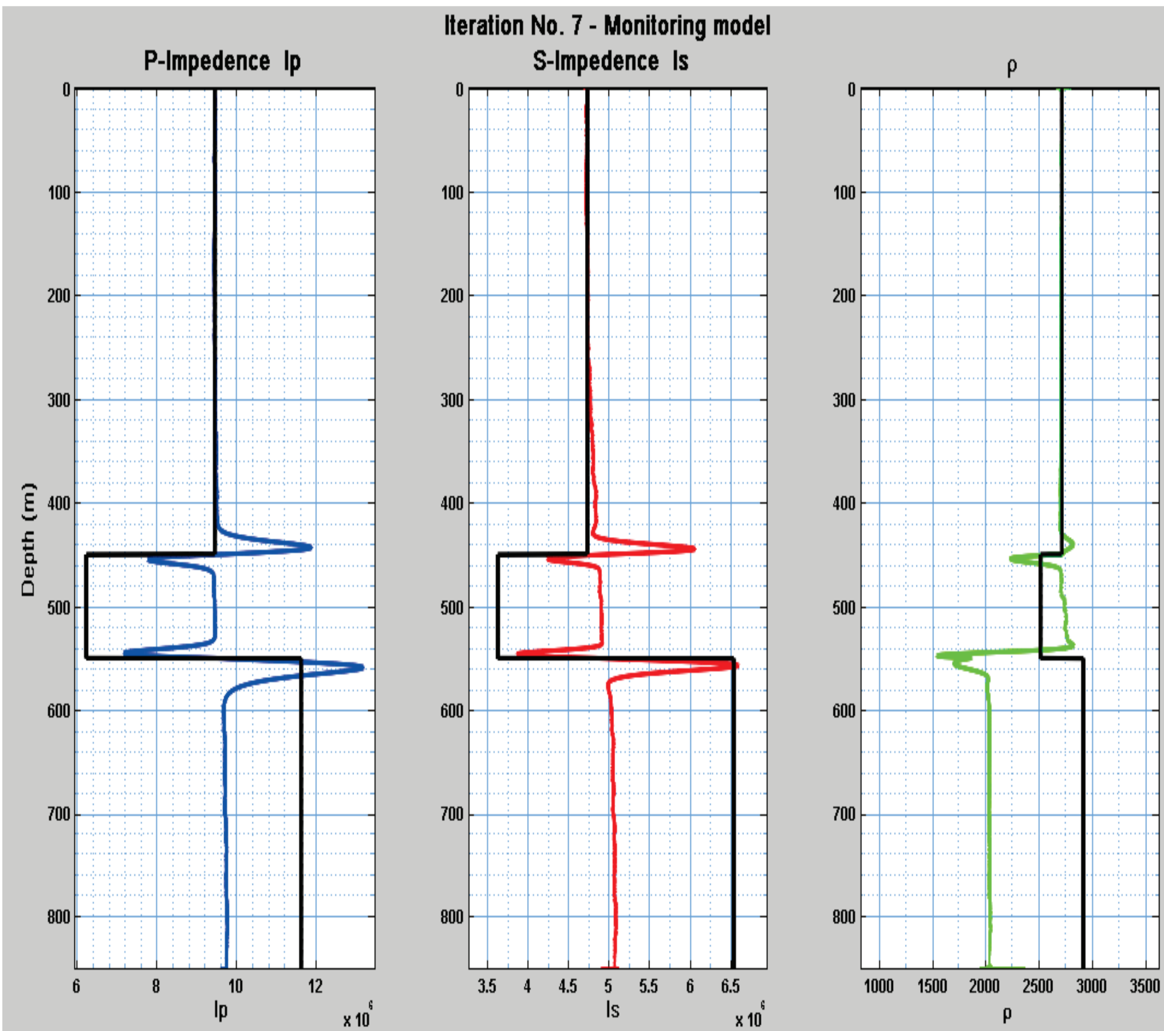

FIG.5. measured and inverted acoustic impedances for the monitor (1) using cross-reflectivity constraint Inversion scheme.

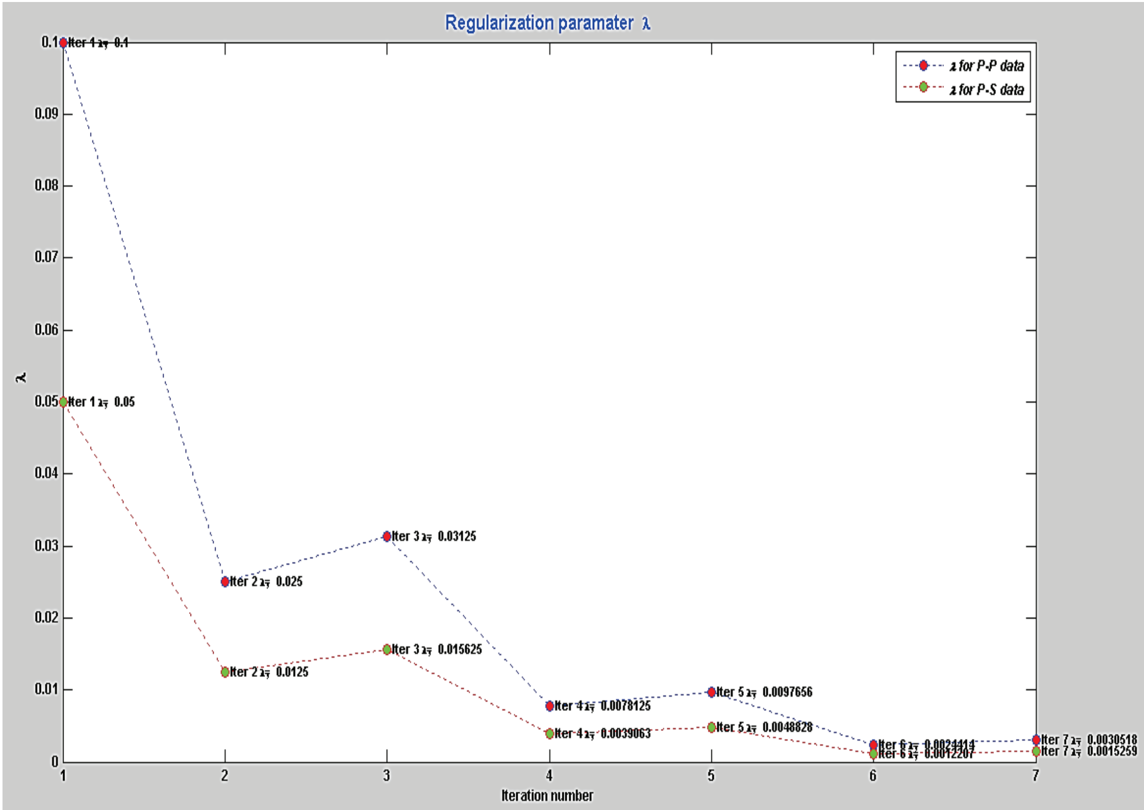

FIG.6. Regularization parameter during cross-reflectivity constraint Inversion scheme.

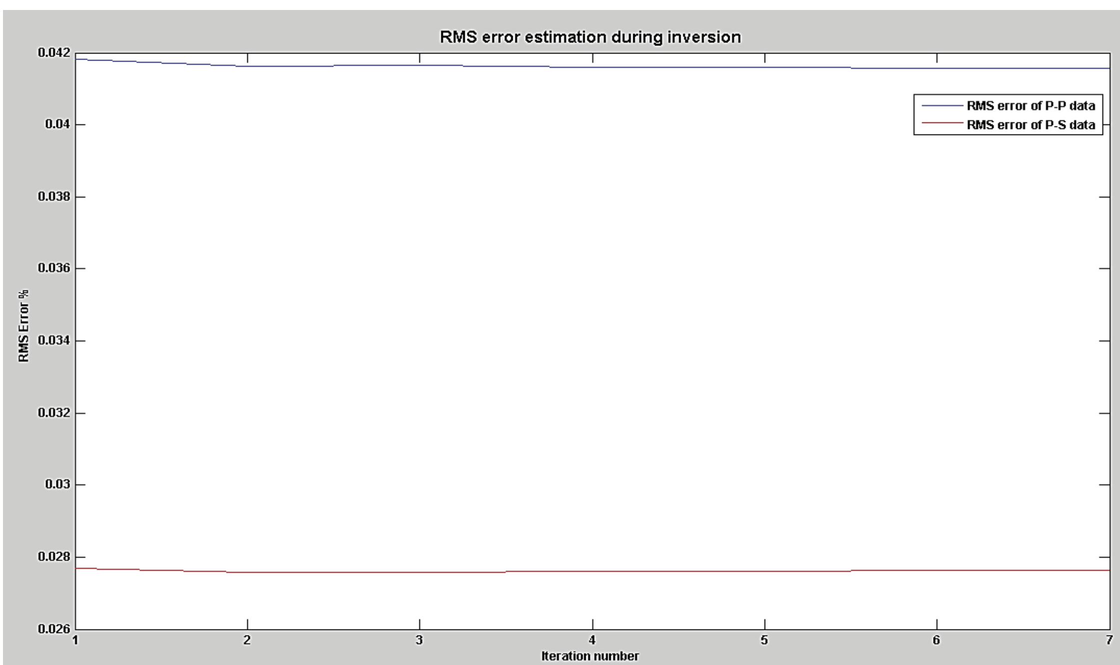

FIG.7. RMS error during cross-reflectivity constraint Inversion scheme.

CONCLUSIONS

Several new inverse schemes for time-lapse AVO inversion are presented in this report. Some of proposed inverse schemes are tested on synthetic data. The developed codes were optimized to perform inversion in less time particularly for robust time-lapse AVO inversion. The accuracy of proposed codes is to be assessed by applying them on real time-lapse seismic data vintages.

FUTURE WORK

The time-lapse seismic data of Pike-Peaks are being processed for AVO complaints and optimal repeatability. The proposed time-lapse AVO inversion techniques in this report are be tested using real time-lapse seismic data from Pike-Peak oil field in order to evaluate their reliability as well as to examine their stability and accuracy.

Estimating of pore pressure and fluid saturation changes are other goals in this research. Possible extension of the research to tackle on anisotropic AVO inversion is being considered.

The final developed computer codes will be compiled in a Matlab GUI for different AVO inversion schemes.

ACKNOWLEDGEMENTS

The authors would like to thank all of the CREWES sponsors for supporting this study.

REFERENCES

Ajo-Franklin, J.B., Minsley B.J. and Daley T.M., 2007, Applying compactness constraints to differential traveltime tomography. Geophysics, **72**, 67-75.

Bube, K.P., and Langan, R.T., 1997, Hybrid lambda1/lambda2 minimization with application to tomography: Geophysics, **62**, 1183-1195.

Claerbout, J.F. and Muir, F., 1973, Robust modeling with erratic data: Geophysics, **38**, 826-844.

Constable, S.C., Parker, R.L., and Constable, C.G., 1987, Occam's inversion: A practical algorithm for generating smooth models from electromagnetic sounding data: Geophysics, **52**, 289-300.

Downton, J.E., 2005, Seismic parameter estimation from AVO inversion: Ph.D. thesis, university of Calgary.

Farquharson, C. G., and Oldenburg, D.W., 1998, Non-linear inversion using general measures of data misfit and model structure: Geophy. J. Int., **134**, 213-227.

Ferguson, R. J., Margrave G.F., 1996, A simple algorithm for band-pass impedance inversion, CREWES Research Report, 8, 1-10.

LandrØ, M., 2001, Discrimination between pressure and fluid saturation changes from time-lapse seismic data: Geophysics, 66, 836-844.

Saeed, A.N., Lines, L.R., and Margrave, G.F., 2010a, Time-lapse AVO inversion: model building and AVA analysis: CREWES report, **22**.

Saeed, A.N., Lines, L.R., and Margrave, G.F., 2010b, Iteratively re-weighted least squares inversion for the estimation of density from well logs: part one: CREWES report, **22**.

Saeed, A.N., Lines, L.R., and Margrave, G.F., 2010c, Iteratively re-weighted least squares inversion for the estimation of density from well logs: part two: CREWES report, **22**.

Watson, I.A. and Lines, L.R., 2001, Time-lapse seismic monitoring at Pikes Peak, Saskatchewan: 2001 CSEG Annual Mtg, Calgary, Alberta.

Wolke, R., and Schwetlick, H., 1988, Iteratively re-weighted least squares algorithms, convergence analysis, and numerical comparisons: SIAM Journal of Scientific and statistical computation, **9**, 907-921.

Zou, Y., 2005, Integration of seismic methods with reservoir simulation, Pikes Peak heavy-oil field, Saskatchewan: Ph.D. thesis, university of Calgary.